Effects of laser beam propagation and saturation on the spatial shape of sodium laser guide stars

Fabien Marc, Hugues Guillet de Chatellus, J. P. Pique

Effects of laser beam propagation and saturation on the spatial shape of sodium laser guide stars

Fabien Marc, Hugues Guillet de Chatellus and Jean-Paul Pique

Laboratoire de Spectrométrie Physique, Université Joseph Fourier, Unité Mixte de Recherche 5588, Centre National de la Recherche Scientifique-Grenoble I,B.P. 87, 38042 Saint Martin d'Hères, France
hguillet@spectro.ujf-grenoble.fr, pique@spectro.ujf-grenoble.fr

Abstract: The possibility to produce diffraction-limited images by large telescopes through Adaptive Optics is closely linked to the precision of measurement of the position of the guide star on the wavefront sensor. In the case of laser guide stars, many parameters can lead to a strong distortion on the shape of the LGS spot. Here we study the influence of both the saturation of the sodium layer excited by different types of lasers, the spatial quality of the laser mode at the ground and the influence of the atmospheric turbulence on the upward propagation of the laser beam. Both shape and intensity of the LGS spot are found to depend strongly on these three effects with important consequences on the precision on the wavefront analysis.

OCIS codes: (010.1080) Adaptive optics; (010.1300) Atmospheric propagation; (010.1330) Atmospheric turbulence; (010.7350) Wave-front sensing; (110.4280) Noise in imaging systems; (110.6770) Telescopes; (140.3295) Laser beam characterization.

References and links

1. F. Roddier (ed.), *Adaptive Optics in Astronomy* (Cambridge Univ. Press, 1999).
2. C. A. Primmerman, D. V. Murphy, D. A. Page, B. G. Zollars, and H. T. Barclay, "Compensation of atmospheric optical distorsions using a synthetic beacon," Nature **353**, 141-143 (1991).
3. L. Thompson and C. Gardner, " Experiments on laser Guide Stars at Mauna Kea Observatory for Adaptive Optics in Astronomy," Nature **328**, 229-231 (1987).
4. A. E. Siegman, *Lasers* (University Science Books, 1986), 206-208.
5. L. Michaille, A. D. Cañas, J. C. Dainty, J. Maxwell, T. Gregory, J. C. Quartel, F. C. Reawell, R. W. Wilson, and N. J. Wooder, "A laser Beacon for monitoring the mesospheric sodium layer at La Palma," Mon. Not. R. Astron. Soc. **318**, 139-144 (2000).
6. O. Lai, C. Veillet, D. Salmon, K. Ho, M. R. Baril, G. A. Barrick, J. Thomas, D. Teeple, T. Benedict, J.-P. Pique, and H. Guillet de Chatellus, "VASAO: visible all sky adaptive optics: a new adaptive optics concept for CFHT," Proc. SPIE **7015**, 701543 (2008).
7. C. d'Orgeville, B. J. Bauman, J. W. Catone, B. L. Ellerbroek, D. T. Gavel, and R. A. Buchroeder, "Gemini north and south laser guide star systems requirements and preliminary designs," Proc. SPIE **4494**, 302-316 (2002).
8. R. Holzloehner, D. Bonaccini Calia, and W. Hackenberg, "Physical Optics Modeling and Optimization of Laser Guide Star propagation," Proc. SPIE **7015**, 701521 (2008).
9. J.-P. Pique and S. Farinotti, "Efficient modeless laser for a mesospheric sodium laser guide star," J. Opt. Soc. Am. B **20**, 2093-2102 (2003).
10. H. Guillet de Chatellus, J.-P. Pique, and I. C. Moldovan, "Return flux budget of polychromatic laser guide stars," J. Opt. Soc. Am. A **25**, 400-415 (2008).
11. A. E. Siegman, *Lasers* (University Science Books, 1986), 626-697.
12. http://www.aor.com/
13. A. N. Kolmogorov, "Dissipation of energy in a locally isotropic turbulence," Dokl. Akad. Nauk SSSR **32**, 16-18 (1941), English translation in Proc. R. Soc. Lond. A **434**, 15-17 (1991).
14. F. Roddier, "The effects of atmospheric turbulence in optical astronomy," Prog. Opt. **19**, 281-376 (1981)

#99731 - $15.00 USD Received 1 Aug 2008; revised 4 Nov 2008; accepted 17 Nov 2008; published 16 Mar 2009

1. Introduction

The revolution brought by the techniques of Adaptive Optics (AO) has lead to a large amount of astronomic data. AO enables one to compensate for the atmospheric turbulence that imposes otherwise a resolution much lower than the ideal diffraction limit [1]. However these techniques require a bright source of light in the vicinity of the object to observe, to be used as a reference for the adaptive-optics loop. Since bright natural stars are rare especially at the galactic poles a possibility has emerged to create an artificial laser guide star, by means of the Rayleigh scattering of a green or UV laser [2], or by the fluorescence light induced by the resonant excitation of the D_2 line of the mesospheric sodium atoms by a yellow laser [3]. Our study is limited to this latter case.

AO is based on the reconstruction of the wavefront at the input pupil of the telescope, by measuring the local slopes on all sub-pupils of the telescopes. The size of the sub-pupil is closely linked to the Fried parameter r_0: the phase of the wavefront over each sub-pupil can be accurately approximated by a linear function of the spatial x and y variables. Each sub-pupil of the telescope matches a sub-pupil of a wavefront analyzer and the real time measurement of the position of the image of the guide star for each sub-pupil gives access to the values of the local slope of the wavefront, *i.e.* to the reconstruction of the light wavefront over the whole aperture of the telescope.

It is evident that the accuracy on the measurement of the wavefront is linked to the precision of the position of the image of the guide star on each sub-pupil. For a natural guide star, this image is logically diffraction-limited on the scale of a single sub-pupil. But for a laser guide star, things go differently from several perspectives.

1- An AO system as well as a laser projector are optimized and designed for a given r_0. But r_0 varies with time (randomly) and with the observed wavelength ($r_0 \propto \lambda^{6/5}$) [1].

2- The laser light is submitted to atmospheric turbulences during its upward propagation to the mesosphere; the weight of this influence being determined by the ratio of the diameter of the laser beam by r_0. When this ratio is much larger than unity, the laser mode at the mesosphere is strongly distorted and the shape of the LGS is very different from what would be expected by a Fresnel-type calculation of the propagation of the laser mode and shows a speckle pattern. On the contrary when this ratio is smaller than unity, the laser suffers only a linear phase shift with x and y, resulting in a lateral global shift of the LGS but without degradation of the spatial shape of the spot.

3- The spatial quality of the laser beam needs to be taken into account: the presence of transverse modes results in a broadening of the laser spot at the mesosphere, compared to a strictly TM_{00} laser beam. Moreover, the wavefronts of high power lasers are affected by random turbulences in the laser medium itself.

4- There is no strict correspondence between the shape of the laser spot at the mesospheric sodium layer and the shape of the LGS because the number of photons emitted by the fluorescence of a sodium atom resonantly excited by laser light, is not proportional to the intensity of the laser light itself. Indeed the phenomenon of saturation results in a non-linear dependence of the fluorescence flux with the laser intensity [4]. On a spatial point of view, this phenomenon results also in a broadening of the LGS.

5- The sodium layer is a strongly non homogenous medium and has a non negligible thickness (~10 km) compared to its distance to the earth (~90 km) [5]. Considering that all sodium atoms are contained in a zero vertical extension layer is actually justified for sub-pupils located next to the axis of emission of the laser beam, for which the elongation of the LGS spot is negligible. Nevertheless for sub-pupils located far away from the laser axis, the vertical structure of the sodium layer should be considered to account for the elongation of the LGS spot. Moreover, the effect of the evolution of the beam size and shape along the 10 km sodium layer should also be considered [6].

In this paper we propose to focus numerically on two sources of degradation of the LGS and study their relative incidence on the shape of the LGS under realistic conditions: the beam propagation through the atmosphere and the non-linear response of the laser induced

#99731 - $15.00 USD Received 1 Aug 2008; revised 4 Nov 2008; accepted 17 Nov 2008; published 16 Mar 2009

fluorescence of sodium atoms. The sodium layer properties and the return fluorescence through the atmosphere and instruments are not discussed in this paper. In the first part, we detail the frame of the study and the methodology we use. In Part II, we treat the case of a Gaussian laser mode at the mesosphere, to evidence the influence of the saturation on the LGS. In Part III we introduce other sources of degradation of the LGS spot: namely the influence of the spatial mode of the laser at the ground by showing the influence of two different values of M^2 on the LGS spot, and the influence of atmospheric turbulence encountered by the laser beam propagating to the sky by considering different values of r_0. In Part IV we show that these causes of spatial broadening of the LGSs also affect notably the total intensity of the LGS.

2. Methodology overview

The characterization of the LGS in terms of spot size and intensity is structured in two steps. First we compute the propagation of the laser beam to the mesosphere across the turbulent atmosphere as a function of the spatial quality of the laser beam, and the Fried parameter. In a second step starting from the spatial distribution of the laser intensity at the mesosphere we calculate the response of the mesospheric sodium layer in terms of fluorescence emission (see Fig. 1).

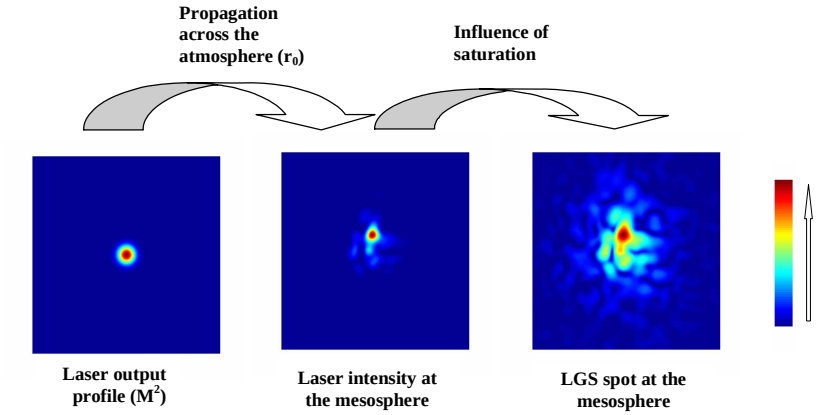

Fig. 1. Methodology of the present study. The calculation is based on two steps: i) propagation of the laser beam to the mesosphere, ii) calculation of the fluorescence spot (i.e. LGS) from the laser intensity spot. The size of each map is 300cm x 300cm. Data are normalized according to the color scale (right).

2.1 Step 1: propagation of the laser beam to the mesosphere

The computation of the laser beam to the mesosphere depends on both laser and atmospheric parameters. Among the different possibilities in terms of technical laser specifications for the production of LGS, pulsed lasers show interesting possibilities compared to CW lasers. Namely it is easier to build a pulsed LGS system since high power pulsed pump lasers are commercially available. From the astronomer's point of view, pulsed format also enable promising time gating applications [7]. The case of CW lasers in the linear regime has been treated very recently [8]. In this paper, we restrict the laser format to 50 ns long laser pulses, with a typical energy in the range 0.05 to 2 mJ corresponding to 18 to 740 kW/m^2 peak intensity in the beam center (for a diffraction-limited beam at the mesosphere). With a repetition rate of 10 kHz, this corresponds to average powers in the range 0.5 W to 20 W at the mesosphere. This laser format is typically what is obtained with dye amplifiers pumped by pulsed green lasers. We choose to study the case of linearly polarized lasers and we assume three types of spectral profiles: single mode, phase-modulated or modeless lasers [9]. Both the

#99731 - $15.00 USD Received 1 Aug 2008; revised 4 Nov 2008; accepted 17 Nov 2008; published 16 Mar 2009

single mode and the phase-modulated lasers are centred on the F=2 lobe of the D_2 line, whereas the modeless laser has a 3 GHz broad continuous spectrum covering the whole D_2 line (see Fig. 2).

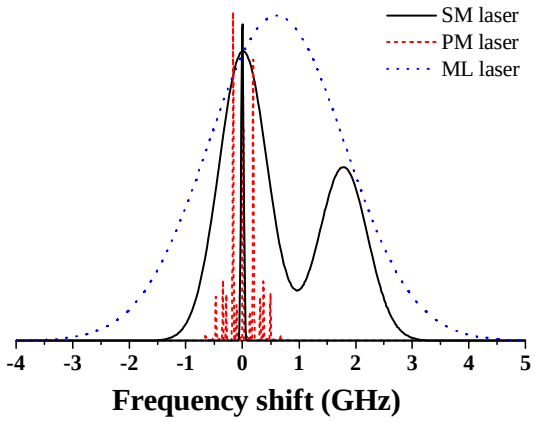

Fig. 2. Laser spectra considered in this study. SM, PM and ML stand respectively for single mode, phase modulated and modeless lasers. The parameters of the phase modulation function are given in [10]. The black solid line is the profile of the sodium D_2 line at the temperature of the mesosphere.

The quality of a laser beam is usually characterised by its M^2. The mathematical definition of M^2 is [11]:

$$M^2 = \frac{\pi r_{1/e^2}\theta}{\lambda} \tag{1}$$

where r_{1/e^2} is the radius at $1/e^2$, θ the half divergence and λ the wavelength of the laser beam (589 nm).

The radial second moment of any 2D intensity distribution is:

$$\sigma(I)^2 = \frac{\int_{-\infty}^{+\infty}\int_{-\infty}^{+\infty} I(x,y)[(x-x_0)^2+(y-y_0)^2]dxdy}{\int_{-\infty}^{+\infty}\int_{-\infty}^{+\infty} I(x,y)dxdy} \tag{2}$$

A TM_{00} beam has a radial amplitude distribution:

$$A(x,y) = A_0 e^{-\frac{x^2+y^2}{r^2_{1/e^2}}} \tag{3}$$

and an intensity distribution:

$$I(x,y) = A(x,y)A^*(x,y) = I_0 e^{-2\frac{x^2+y^2}{r_{1/e^2}{}^2}} = I_0 e^{-\log(2)\frac{x^2+y^2}{r_{1/2}{}^2}} \tag{4}$$

$r_{1/2}$ is the radius at half maximum (HWHM). We have:

$$r_{1/e^2} = r_{1/2}\sqrt{\frac{2}{\log(2)}} \tag{5}$$

#99731 - $15.00 USD Received 1 Aug 2008; revised 4 Nov 2008; accepted 17 Nov 2008; published 16 Mar 2009

In the following we use the surface *S* at half maximum:

$$S = \pi r_{1/2}{}^2 \tag{6}$$

The radial second moment of a pure TM_{00} beam is then:

$$\sigma(I) = \frac{r_{1/e^2}}{2} = \frac{r_{1/2}}{\sqrt{2\log(2)}} \tag{7}$$

To summarize, the second moment applied to the radial distribution gives the waist r_{1/e^2}. The second moment applied to the angular distribution (intensity distribution in the frequency domain) gives the divergence θ. Then, M^2 can be calculated using the formula above. Note that M^2 does not characterize a single beam; several different beams may have the same M^2.
In the present study we consider two situations corresponding to different values of M^2: a perfect TM_{00} mode (M^2 = 1) and a slightly degraded laser mode characterized by M^2 = 1.3. This value corresponds to very good available lasers. A larger value would not be suitable for LGS applications, since the size of the laser spot at the mesosphere would be too large, and degrade the precision of the measurement of the wavefront. Such M^2 values are achievable in amplified dye laser systems. We also suppose that the laser beam is launched to the mesosphere by a 50 cm diameter telescope corrected from spherical aberrations. The size of the laser beam has been chosen to 15 cm at the ground (radius at $1/e^2$), *i.e* to 8.85 cm (HWHM).

The propagation to the mesosphere is computed by mean of the GLAD software (version 5.2) [12]. The algorithm is based on scalar Fresnel diffraction theory.
First, the wavefront profile is sampled on a 512×512 grid, the total size being 300 cm×300 cm. The amplitude of the laser beam is sampled according to a spherical gaussian distribution, with a waist r_{1/e^2} = 15 cm (i.e. $r_{1/2}$ = 8.85 cm).

Using the GLAD random-phase command, we add a smoothed Gaussian random wavefront aberration to the beam which simulates turbulences inside the amplifier medium and which leads to a M^2 larger than 1. With the different parameters of this function (wavefront error waves RMS, and autocorrelation radius), we adjust our beam to an average M^2 equal to 1.3. In this case, we consider 10 different cases of random phases.

Atmospheric aberrations are added according to Kolmogorov model [13]. The power spectrum of the wavefront is:

$$W^2(\rho) = \frac{0.023 e^{-\rho^2 L_i^2}}{r_0^{5/3}\left(\rho^2 + \frac{1}{L_0^2}\right)^{11/6}} \tag{8}$$

where ρ is the spatial frequency, L_0 is the outer scale and L_i is the inner scale. L_0 can be considered as the scale of the motions which give rise to turbulence and L_i as the scale at which viscous dissipation arises. According to [14], we consider the typical atmospheric values L_0 = 10 m and L_i = 1 mm as input parameters in the code. To characterize different atmospheres we choose the following Fried's parameters at 589 nm: 5 cm, 10 cm, and infinite (no turbulence). The case 10 cm is obtained at very good astronomical sites like Mauna Kea. To do this study, we consider 50 random cases of atmosphere (for a given set of L_0, L_i and r_0). Then, the beam is propagated though this atmosphere over 90 km using GLAD's propagator, which returns the laser intensity map at the mesosphere. This propagation corresponds to pointing the laser at the zenith.

2.2 Step 2: production of the LGS spot

The laser intensity map at the mesosphere (at 90 km) is then converted into a grid giving the intensity in Watts per cm^2. In a previous publication, we investigated the efficiency of both

#99731 - $15.00 USD Received 1 Aug 2008; revised 4 Nov 2008; accepted 17 Nov 2008; published 16 Mar 2009

monochromatic and polychromatic LGS by means of both a rate-equations model and a Bloch equation code for top-hat or Gaussian beam profiles at the mesosphere [10]. These numerical models link the laser intensity per surface unit to the probability of spontaneous emission per sodium atom for the three types of lasers considered in this study. A laser intensity map can therefore be converted into a fluorescence map, giving the number of fluorescence photons emitted by a single sodium atom per steradian, depending on its location on the grid. The fluorescence map gives actually the profile of the LGS spot at the mesosphere. These models neglect the effect of the Earth's magnetic field.

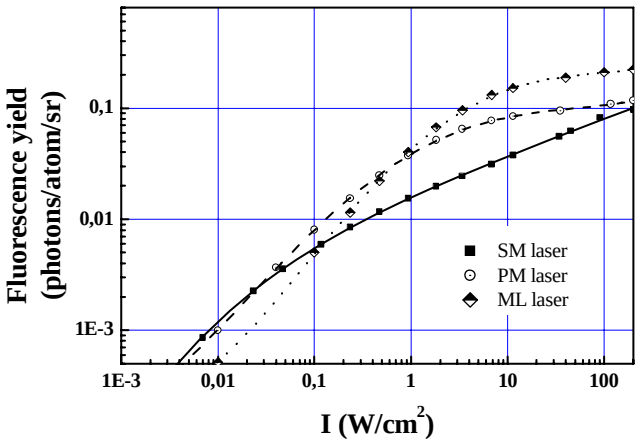

Fig. 3. Number of photons emitted per steradian, per sodium atom and per laser pulse as a function of the laser power density for different laser types (50 ns pulse duration, linear polarization). The numerical values are given by the density matrix code Beacon [10].

It is clear from Fig. 3 that the response of the sodium atom in terms of fluorescence signal is nonlinear with respect to the laser power. This evidences the phenomenon of saturation in atomic fluorescence which corresponds to the fact that after the atom has been transferred into the excited state (lifetime 16ns) by absorption of a resonant photon, another laser resonant photon induces the stimulated emission of a photon having the same wave vector as the laser photon [4]. This is particularly problematic for LGSs, where one detects the return fluorescence. Saturation leads to a non-linear dependence of the sodium fluorescence with the laser power density. Of course, saturation affects mostly LGS created by pulsed lasers compared to CW lasers because of the higher peak power involved.
Concerning the intensity of the LGS per laser pulse and considering that the transmission of the atmosphere is 100%, the number of photons received by the telescope per square meter is:

$$\Phi = \frac{d_{Na} s}{D^2} \sum_{i=1}^{512} \sum_{j=1}^{512} n(i, j) \qquad (9)$$

where:
- Φ (in photons/s/m^2) is the return flux per second and per m^2 of telescope.
- d_{Na} is the surface sodium density in the mesosphere ($d_{Na} = 4.10^{13}$ atoms/m^2).
- s is the size of a single pixel of the grid ($s = (3/512)^2 = 3.43\ 10^{-5}$ m^2).
- D is the distance from the ground level to the mesosphere ($D = 90.10^3$ m).
- $n(i, j)$ is the number of photons emitted per steradian and per laser pulse by a sodium atom located in the pixel *(i,j)* of the grid.

#99731 - $15.00 USD Received 1 Aug 2008; revised 4 Nov 2008; accepted 17 Nov 2008; published 16 Mar 2009

3. Spatial shape of the LGS induced by a TM00 gaussian laser mode at the mesosphere

Here we study the simple case of a laser beam supposed TM_{00} at the mesosphere without turbulence. In this case we quantify specifically the influence of the saturation of the sodium atom by the laser beam. This situation could also be experimentally implemented by using high order adaptive optics on the laser launch telescope to restore at the mesosphere level, the diffraction-limited Gaussian mode of the laser. A simple calculation shows that a laser beam having a radius at 1/2 equal to 8.85 cm at the ground (*i.e.* 0.025 m^2) leads to a laser spot at the mesosphere having a size of 11.1 cm (radius at 1/2), and a surface of 0.039 m^2.

3.1 Broadening of the LGS spot

We define the fluorescence spot broadening as the ratio: $\frac{S_{fluo}}{S_{laser}}$ where S_{fluo} is the surface of the fluorescence spot (LGS) and S_{laser} the surface of the laser spot. The surfaces are calculated with the process described in paragraph 1.1.2. In Fig. 4 we compare typical broadening with different laser type. We note that the broadening can reach large values (between 2 and 5) for 1 mJ-single mode or phase-modulated laser pulses.

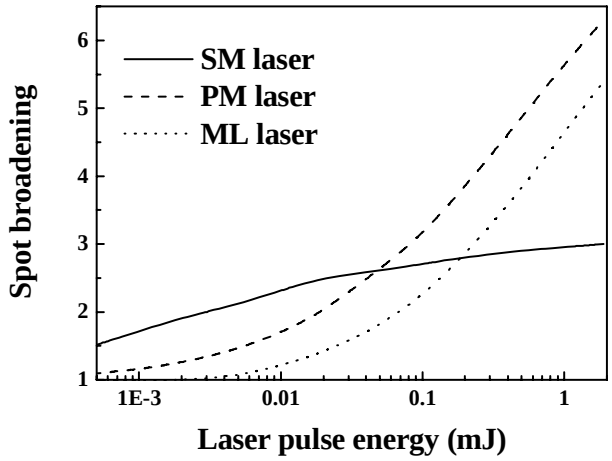

Fig. 4. Evolution of the spot broadening with the laser power for different laser formats (SM: single-mode, PM: phase modulation and ML: modeless laser).

3.2 Figure of merit of the LGS in the Gaussian case

To compare different laser solutions in terms of AO applications, it is interesting to define a figure of merit for the LGS. Indeed on one side it is desirable to create a small LGS –it gives a better precision on the monitoring of the LGS, and on the other side a decrease of the size of the laser spot results in a decrease of the return flux because of the saturation. There is a trade-off between the size of the laser spot and the return flux. A possible figure of merit has been conveniently defined as Φ / S_{fluo}, where Φ is the total return flux, and S_{fluo} is the surface of the fluorescence spot [10]. In Fig. 5 we plot the value of this parameter (in arb. units) with respect to the laser pulse energy, for different laser types. First it is interesting to notice that the figure of merit increases with the laser power for all types of lasers. This simply shows that increasing the laser power results in a larger flux and the benefit of this increase of the return flux dominates over the loss coming from the spot broadening due to the saturation. It is also

#99731 - $15.00 USD Received 1 Aug 2008; revised 4 Nov 2008; accepted 17 Nov 2008; published 16 Mar 2009

worth noting that a modeless spectrum shows the best performances, over single mode or phase modulated lasers.

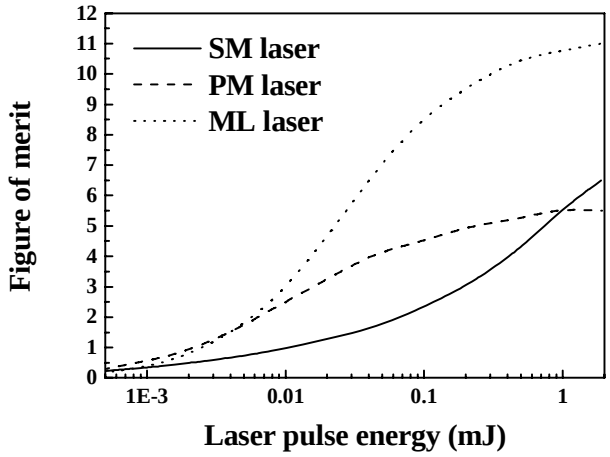

Fig. 5. Variation of the figure of merit of the LGS with the laser power for different laser format (SM: single-mode, PM: phase modulation and ML: modeless laser).

4. Influence of the laser mode and of the atmospheric turbulence on the shape of the LGS

4.1 Numerical treatment

In this part we extend the results obtained in the case of a Gaussian laser TM_{00} mode at the mesosphere to the real-case situation where the laser mode is not ideal and where the atmosphere is turbulent. Our calculations are based on numerical simulations performed with GLAD. The values we consider here for r_0 are 5 cm, 10 cm and infinity. A statistical treatment is carried out to account for the statistical nature of atmospheric turbulence: for r_0 = 5 cm and 10 cm, 50 different atmospheric turbulences maps are computed. Concerning the laser profile, we consider both M^2 =1 (ideal Gaussian mode) and M^2 = 1.3. In the latter case, 10 laser wavefront maps are considered for each simulation to account for the fact that the value of the M^2 does not uniquely characterize the wavefront. And finally to take the saturation effect into account, 6 different laser powers are considered: 0.05, 0.1, 0.2, 0.5, 1 and 2 mJ per pulse. These situations are summarized in Table 1.

Table 1. Summary of the different simulations performed for an accurate statistical treatment for each laser type (SP, PM and ML) and each pulse energy (0.05, 0.1, 0.2, 0.5, 1 and 2 mJ). The pulse width is fixed to 50 ns.

	M^2 = 1	M^2 = 1.3
$r_0 = \infty$	1 atm. x 1 phase map	1 atm. x 10 phase maps
r_0 = 10 cm	50 atm. x 1 phase maps	50 atm. x 10 phase maps
r_0 = 5 cm	50 atm. x 1 phase maps	50 atm. x 10 phase maps

4.2 Broadening of the LGS spot

First we consider the case where the laser M^2 is equal to 1. This enables to quantify the influence of the atmospheric turbulence on the size of the LGS for various laser energies and spectra. Results are presented in Fig. 6. The fluorescence spot size is calculated according to

#99731 - $15.00 USD Received 1 Aug 2008; revised 4 Nov 2008; accepted 17 Nov 2008; published 16 Mar 2009

paragraph 1.1.2 and the radius at half maximum (HWHM) is plotted as a function of the laser pulse energy. In the conditions of non-turbulent atmosphere (r_0 infinite) and of minimal saturation (*i.e.* weak laser energy and modeless laser), the HWHM tends logically to 11.1 cm (black data). When the atmospheric turbulence in taken into account (red and green data), an important broadening is observed. In the limit of very strong saturation (SM laser, 2 mJ) and turbulent atmosphere (r_0 = 5 cm), the surface broadening can reach a factor of ~40. For a given set of laser power and a finite r_0, the modeless laser always leads to the smallest broadening, the largest one corresponding to the single-mode laser.

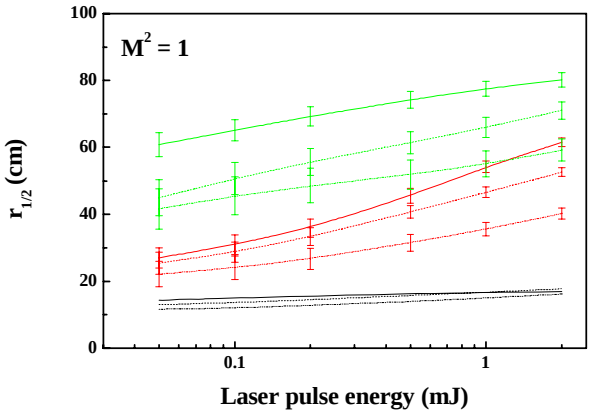

Fig. 6. Variation of the HWHM of the LGS spot with the laser pulse energy for a laser with M^2 =1. Solid lines: single mode laser, dashed lines: phase-modulated laser, dotted lines: modeless laser. Green data: r_0 = 5 cm, red data: r_0 = 10 cm and black data: r_0 infinite. Error bars correspond to the standard deviation of the data defined in Table 1.

Then we study the case of a laser having a slightly degraded wavefront (M^2 = 1.3). The numerical results are presented on Fig. 7. Note that curves are quite similar to the case M^2 = 1: the degradation of the wavefront results in a relatively small broadening of the LGS compared to the Gaussian case. The main causes of broadening remain the saturation (laser power) and the atmospheric turbulence.

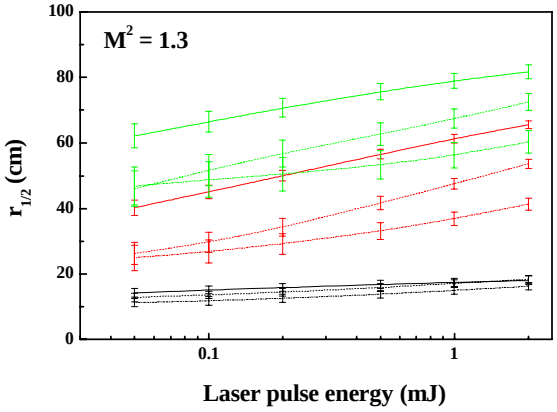

#99731 - $15.00 USD Received 1 Aug 2008; revised 4 Nov 2008; accepted 17 Nov 2008; published 16 Mar 2009

Fig. 7. Variation of the HWHM of the LGS spot with the laser pulse energy for a laser with M^2 =1.3. Solid lines: single mode laser, dashed lines: phase-modulated laser, dotted lines: modeless laser. Green data: r_0 = 5 cm, red data: r_0 = 10 cm and black data: r_0 infinite. Error bars correspond to the standard deviation of the data defined in Table 1.

5. Influence of the atmospheric turbulence and of the laser mode on the intensity of the LGS

In the last part of the paper, we study the intensity of the LGS under realistic conditions: turbulent atmosphere and non-gaussian laser mode. In the previous parts we evidenced that these two factors are important sources of the fluorescence spot broadening compared to a diffraction limited Gaussian laser spot. Since the spot is broadened, the intensity of the LGS is expected to increase because the saturation is decreased by the broadening. Here we study successively the influence of the r_0 on the return flux induced by a Gaussian TM_{00} laser beam and the influence of the M^2 in the case where r_0 is infinite.

5.1 Influence of r_0

We consider a Gaussian laser TM_{00} mode at the mesosphere and we calculate the number of photons per laser pulse received per m^2 of telescope. This number is logically found to increase with the laser power. For a given value of r_0 and a given laser pulse energy the highest return flux is obtained for the modeless excitation. For a given laser type and a given pulse energy, the return flux increases strongly when the r_0 decreases. For instance in the case of a single mode laser delivering 2 mJ pulses, the return flux when r_0 = 5 cm is multiplied by a factor of 5 compared to the case where r_0 is infinite (see Fig. 8).

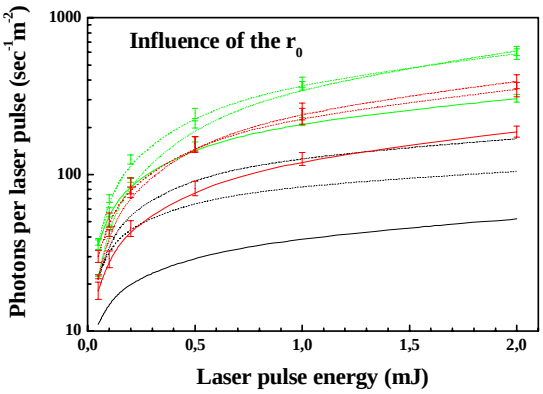

Fig. 8. Variation of the intensity of the LGS spot with the laser pulse energy for a laser with M^2 =1. Solid lines: single mode laser, dashed lines: phase-modulated laser, dotted lines: modeless laser. Green data: r_0 = 5 cm, red data: r_0 = 10 cm and black data: r_0 infinite.

5.2 Influence of the laser M^2

In this paragraph we ignore the distortion by the atmosphere (i.e. r_0 infinite) and focus on the influence of the laser M^2 on the return flux. We compare the number of photons per laser pulse received per m^2 of telescope for different laser formats and powers, when the laser M^2 is degraded from 1 to 1.3. Results are presented on Fig. 9. We observe that the return flux increases because of the spreading of the laser spot at the mesosphere, saturation is reduced and the return flux is enhanced. Note however that the increase in the return flux does not exceed 20 %.

#99731 - $15.00 USD Received 1 Aug 2008; revised 4 Nov 2008; accepted 17 Nov 2008; published 16 Mar 2009

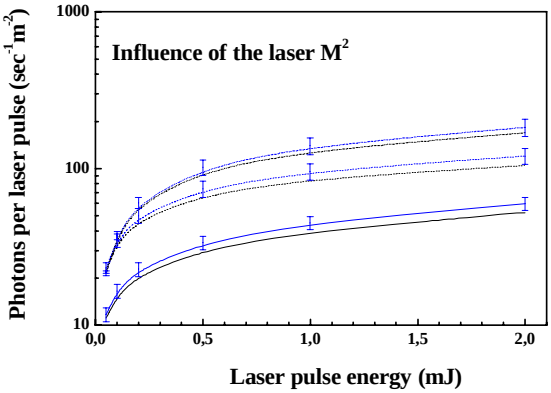

Fig. 9. Variation of the intensity of the LGS spot with the laser pulse energy for a laser for M^2 =1 (black) and M^2 = 1.3 (blue). r_0 is infinite. Solid lines: single mode laser, dashed lines: phase-modulated laser, dotted lines: modeless laser.

The influence of the laser mode is therefore found to be small compared to the influence of the atmospheric turbulence.

6. Conclusion

The results obtained in this study are important from a triple point of view. We evidence and quantify the phenomenon of broadening of the LGS due to several factors: the saturation of the sodium atom by the laser, the atmospheric turbulence and the quality of the laser mode. The evaluation of the broadening of the LGS depends on the criteria used to characterize the surface. Taking into account the surface at half-maximum the results for 2 mJ laser pulses can be summarized in the Table 2: we give the surface broadening, defined by the ratio of the surface at half-maximum divided by 0.039 m^2, the surface corresponding to a diffraction limited Gaussian beam at the mesosphere.

Table 2. Surface broadening for 2mJ/50ns laser pulses for different laser formats and seeing conditions.

		r_0 infinite	r_0 = 10 cm	r_0 = 5 cm
M^2 = 1	SM	2.6	31	52
	ML	2.1	13	29
M^2 = 1.3	SM	2.8	35	55
	ML	2.2	14	30

This work also links the broadening of the LGS with an increase of the intensity of the LGS, because of the de-saturation brought by the spatial broadening. In Table 3 we recall the number of return photons seen per laser pulse and per m^2 of telescope, for a pulse intensity of 2 mJ.

Table 3. Return flux at the ground per m^2 of telescope produced per 2 mJ laser pulses for different laser formats and seeing conditions. The atmospheric transmission is supposed to be 100%.

		r_0 infinite	r_0 = 10 cm	r_0 = 5 cm
M^2 = 1	SM	52	190	300
	ML	170	390	620
M^2 = 1.3	SM	62	200	310
	ML	180	400	620

#99731 - $15.00 USD Received 1 Aug 2008; revised 4 Nov 2008; accepted 17 Nov 2008; published 16 Mar 2009

Finally this study gives interesting directions for the choice of a LGS system. Saturation has to be reduced since it leads to a broadening of the LGS and a decrease in the return flux. For these two reasons, it is preferable to use a laser spectral line able to excite all velocity classes of mesospheric sodium atoms. Atmospheric turbulence is also an important source of spot broadening but leads to an increase of the return flux. The laser beam quality has the same effects but the influence is less. Therefore the efficiency of a LGS depends strongly on the atmospheric conditions. An important point which has not been evaluated here is the sensitivity of the return fluorescence to atmospheric perturbations and instrumentation aberrations. It is a crucial issue because first, r_0 has a systematic evolution with time and wavelength and second, AO characteristics can never be optimized for every situation. This point will be addressed in a forthcoming paper.

Acknowledgments

This work was supported by the CNRS and the Région Rhône-Alpes (Program CIBLE).

#99731 - $15.00 USD Received 1 Aug 2008; revised 4 Nov 2008; accepted 17 Nov 2008; published 16 Mar 2009